Improved Joint Transform Correlator Performance Through Spectral Domain Thresholding

Thomas Naughton[1], Miloš Klíma[2], and Jiří Rott[2]

[1] Department of Computer Science, National University of Ireland, Maynooth, Ireland. E-mail: tomn@cs.may.ie
[2] Department of Radioelectronics, Faculty of Electrical Engineering, Czech Technical University in Prague, Czech Republic

Abstract. Joint Fourier transform correlation is an analog optical signal processing technique capable of comparing several two-dimensional images. We show that selected spectral domain binary thresholds, obtained through simulation, significantly improve the performance of an optical implementation of the joint transform correlator. In doing so we establish empirically the existence of well defined optimal uniform thresholds for the image classes tested. We also investigate the discrimination capabilities of the linear joint transform correlator, both by simulation and optically, in multiple input environments.
Keywords: optical pattern recognition; binary joint transform correlator; spectral domain processing; optimal thresholding.

1 Introduction

The joint Fourier transform correlation technique [24] is one of the most frequently applied methods in the field of optical object recognition and classification. One of the many modifications to the conventional, or linear, joint transform correlator (JTC) involves binarisation [12, 13] of the frequency power spectrum after the first Fourier transform. Currently, there is no general solution to the problem of identifying an input image's optimal uniform threshold level when binarising its power spectrum. In this paper we call this the optimal threshold problem.

Previously [15], we have quantified the rotation and scaling tolerances of the linear JTC with various inputs of differing spatial character. These tolerances will be used to quantify any gains made through spectral domain thresholding. In [15] we also investigated (through simulation) both uniform and exponential thresholding in the spectral domain of a binary JTC (BJTC) for a class of fingerprint images.

We continue in this paper by firstly showing through simulation that a well defined optimal uniform threshold exists for each of our database of images, and secondly verifying those thresholds by optical experiment. This has been done with a view to finding a general solution to the optimal threshold problem. In the

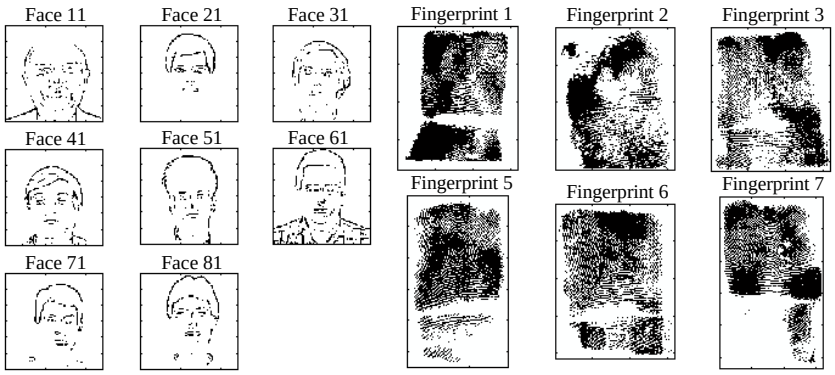

Fig. 1. The two image classes used in experiments: faces and fingerprints

experiments we use two image classes with fundamentally different spatial characteristics (fingerprints and faces), shown in Fig. 1. Although the choice of image sets was not arbitrary, issues relating to biometric recognition are not addressed here. We have simply chosen two (albeit binary) image sets which have visibly different image characteristics in terms of total power and spatial frequency composition in order to investigate the interclass and intraclass differences between each optimal threshold found.

The uniform thresholds were found to improve the BJTC's performance over both image classes. After isolating the optimal threshold level for a particular image, our BJTC exhibited significantly higher and better resolved cross-correlation peaks and superior signal to noise ratios than the linear (unthresholded) JTC.

Finally in this paper, we determine the extent of the linear JTC's ability to discriminate between multiple inputs in order to accurately quantify (in the future) the increased intraclass discrimination capabilities of an optimally thresholded multichannel BJTC.

2 Background

Pattern recognition is one of the most commonly implemented signal and image processing tasks. A significant number of the digital electronic solutions proposed for pattern recognition problems involve a convolution operation, such as to correlate two images on a pixel-by-pixel basis (e.g. template matching) or to pre-process an image (e.g. edge detection prior to applying a Hough transform [11]). The concept of pattern recognition effected through *optical* correlation is closely related to the information processing technique of optical spatial frequency filtering [6, 19, 20]. The theory of optical filtering is both mature and well researched, and it has been shown that not only are optical pattern recognition systems possible [4], but also that the inherent parallel nature of optical systems can be used to facilitate low time- and space- computational complexity

implementations of the correlation operation. If *reliable* optical pattern recognition techniques can be perfected they may prove to be invaluable tools to the image processing community and to the greater signal processing community.

A promising example would involve the optical correlator being used as a front end to a generalised hybrid object recognition system. The optical component would quickly and efficiently identify regions of interest in a cluttered scene and pass these on to the slower but more accurate (and of course programmable) digital electronic components for false-alarm reduction, feature extraction and classification.

Two-dimensional optical correlators have been in existence since the 1950s [2]. These initial systems performed optical Fourier transforms and recognised patterns by means of spatial filtering. Today, in the field of analog optical processing, spatial filter-based correlation (such as matched filtering) and joint Fourier transform correlation are the two most widely applied optical pattern recognition techniques [8].

2.1 Matched Filtering

Optical spatial filtering involves altering the frequency content of an image by placing filters in the Fourier plane of a 2-D (two dimensional) SLM (spatial light modulator) encoding that image. When this filter H is a function of the complex conjugate of the reference image's frequency domain representation S,

$$H(\alpha, \beta) = S^*(\alpha, \beta) \ , \tag{1}$$

we call it a matched filter, where α and β define the spatial frequency domain and * denotes the complex conjugate. When the matched filter of a sought object is multiplied by the frequency spectrum F of an input signal f containing that object, and a Fourier transform taken of the product,

$$f \circledast s = \mathcal{F}^{-1}\Big\{F(\alpha, \beta)H(\alpha, \beta)\Big\} \ , \tag{2}$$

a strong correlation peak is produced in the output (correlation) plane. Here, $\circledast$ denotes the correlation operation and $\mathcal{F}^{-1}$ signifies the application of an inverse Fourier transform. This follows from the well-known theory that a space domain convolution may be represented by an equivalent frequency domain multiplication.

Matched filtering allows reliable detection of signals in the presence of noise (white-noise, in the simplified case of (1)). VanderLugt [21] proposed and demonstrated a practical technique for representing these complex matched filters with a purely amplitude modulating SLM. These practical filters have subsequently become known as VanderLugt filters.

Apart from its many positive aspects, pattern recognition through matched filtering has several significant drawbacks. Principal among these are low tolerances [22] to misalignment of the two frequency spectra F and H of (2), and the necessity to know all reference images in advance in order to construct their

spatial filters. It is possible to overcome these drawbacks with a technique known as joint Fourier transform correlation [24]. Instead of directly multiplying two frequency spectra to effect correlation, as the matched filter does, we square the sum of two frequency spectra. A conversion back to the spatial domain gives us an equivalent result (see (4) through (6)).

3 The Joint Transform Correlator

The Fourier equations defining the joint transform correlator describe an image processing system with the ability to quantify the degree of similarity between several images or to discriminate between multiple objects in the input plane.

3.1 An Autocorrelation System

To begin with, one could describe the JTC as a system which performs an autocorrelation of its input. This capability in itself does not seem very exciting until we realise that this input plane may be composed of several images. An autocorrelation of the plane will perform a cross-correlation operation on each combination of images. Figure 2 shows the spatial relationship between an input plane composed of two images and the corresponding correlation output.

The positions of the correlation peaks in the output plane are uniquely determined by the configuration of images in the input plane. Quantifying the result of a particular cross-correlation will therefore not involve a search for the appropriate peak in 2-D correlation space (as it might seem to the casual observer) but will simply require calculation of the location of the peak and a single point measurement. Furthermore, spatially fixing the positions of the images in the input plane will ensure that the appropriate cross-correlation terms are always spatially fixed in the output plane, permitting the cross-correlation peak location to be calculated once and stored.

It is possible to effect normalised cross-correlation [23] by a straightforward comparison with the correlation plane's dc term. This component, at the origin, represents the autocorrelation of the complete input plane, thus giving an indication of the combined power of the reference and input signals.

3.2 Operation

The JTC is based on two successive Fourier transforms with some intermediate nonlinear processing (a squaring operation in the conventional, or 'linear', JTC). Its basic operation is illustrated in Fig. 2. Both input image s and reference image r (we imagine there are just two for the moment) are coplanar

$$f(x, y) = s(x, y) + r(x, y) \ . \tag{3}$$

They are Fourier transformed concurrently, so that both frequency spectra are also coplanar. If both images are aligned rotationally (a trivial task if we encode

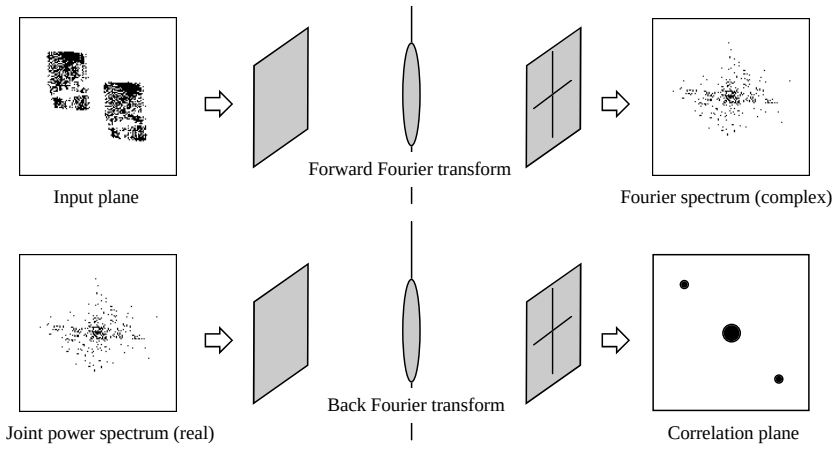

Fig. 2. Illustration of the flow of information in the joint transform correlator, showing the spatial relationship between the distribution of energy in the input and correlation planes

them side-by-side on a single SLM) then we are guaranteed (equipment quality permitting) that there will be no misalignment between the two frequency spectra.

Instead of multiplying the two frequency spectra as the matched filter does, a complex addition of the spectra appears at their common Fourier plane. This follows from the Fourier transform linearity (or addition) theorem [3] which states that the transform of a sum of several spatial functions is a superposition of their frequency spectra. This natural phenomenon, interference, is expressed

$$\begin{aligned} F(\alpha,\beta) &= \mathcal{F}\Big\{s(x,y)+r(x,y)\Big\} = \mathcal{F}\Big\{s(x,y)\Big\}+\mathcal{F}\Big\{r(x,y)\Big\} \\ &= S(\alpha,\beta)+R(\alpha,\beta)\ . \end{aligned} \tag{4}$$

Intuitively, from the matched filtering definition in Sec. 2.1, we know that a convolution of two signals must entail some sort of multiplication of their frequency spectra. The multiplication is accomplished at this point by squaring the absolute value of the complex interference pattern, producing an intensity distribution known as a joint power spectrum

$$\begin{aligned} I(\alpha,\beta) &= \big|F(\alpha,\beta)\big|^2 = \big|S(\alpha,\beta)+R(\alpha,\beta)\big|^2 \\ &= \big|S(\alpha,\beta)\big|^2+\big|R(\alpha,\beta)\big|^2+2\big|S(\alpha,\beta)R(\alpha,\beta)\big|\ . \end{aligned} \tag{5}$$

Squaring the absolute value of a complex function is equivalent to multiplying it by its complex conjugate, so (5) becomes

$$\begin{aligned} I(\alpha,\beta) = {} & S(\alpha,\beta)S^*(\alpha,\beta)+R(\alpha,\beta)R^*(\alpha,\beta) \\ & +S(\alpha,\beta)R^*(\alpha,\beta)+S^*(\alpha,\beta)R(\alpha,\beta)\ . \end{aligned} \tag{6}$$

Since $S(\alpha,\beta)R^*(\alpha,\beta)$ has been formed in this intensity function, the correlation of S and R can be found by obtaining the impulse response of this term. Therefore, an inverse Fourier transform of the complete signal in (6) finds a correlation plane composed of four terms. Two are concentric autocorrelation terms (SS^* and RR^*) and two are cross-correlation terms (SR^* and RS^*). To fully describe the spatial distribution of light in the correlation plane we need to repeat our analysis, this time taking into account spatial shifts in the input plane and working with the phase terms that this will introduce.

3.3 Distribution of Light in the Correlation Plane

Suppose our input signal is composed of two images s and r centred at positions $(-a,+b)$ and $(+c,-d)$, respectively,

$$f(x,y) = s(x-a,y+b) + r(x+c,y-d)\ . \tag{7}$$

The complex light distribution in the spectral plane, as determined from the Fourier shift theorem[1], is

$$F(\alpha,\beta) = S(\alpha,\beta)e^{i2\pi(\alpha a-\beta b)} + R(\alpha,\beta)e^{-i2\pi(\alpha c-\beta d)} \tag{8}$$

and the joint power spectrum becomes

$$\begin{aligned} I(\alpha,\beta) &= \left|S(\alpha,\beta)e^{i2\pi(\alpha a-\beta b)} + R(\alpha,\beta)e^{-i2\pi(\alpha c-\beta d)}\right|^2 \\ &= \left|S(\alpha,\beta)\right|^2 + \left|R(\alpha,\beta)\right|^2 \\ &\quad + S(\alpha,\beta)R^*(\alpha,\beta)e^{i2\pi(\alpha(a+c)-\beta(b+d))} \\ &\quad + S^*(\alpha,\beta)R(\alpha,\beta)e^{-i2\pi(\alpha(a+c)-\beta(b+d))}\ . \end{aligned} \tag{9}$$

A conversion back to the spatial domain with the back Fourier transform (the inverse *optical* Fourier transform) produces the following correlation terms [24]

$$\begin{aligned} g(u,v) &= c_{ss}(u,v) + c_{rr}(u,v) \\ &\quad + c_{sr}(u+a+c,v-b-d) + c_{rs}(u-a-c,v+b+d) \end{aligned} \tag{10}$$

where

$$\begin{aligned} &c_{ss}(u,v) = s(x,y) \circledast s(x,y) && \text{centred at } (0,0), \\ &c_{rr}(u,v) = r(x,y) \circledast r(x,y) && \text{centred at } (0,0), \\ &c_{sr}(u+a+c,v-b-d) = r(-x,-y) \circledast s(-x,-y) \\ &\qquad && \text{centred at } (a+c,-b-d), \text{ and} \\ &c_{rs}(u-a-c,v+b+d) = s(x,y) \circledast r(x,y) \\ &\qquad && \text{centred at } (-a-c,b+d). \end{aligned}$$

[1] We use a positive exponential in both our forward and back optical (spatial) Fourier transforms [18].

The first two terms, the autocorrelation terms, are centred at the origin. This combined signal (the dc term) is of limited use, although it does indicate the total power in the input plane. The third and fourth terms, the cross-correlation terms, are displaced uniformly from the origin. Either one gives us a measure of the cross-correlation between the input and reference images.

3.4 Modifications to the Linear JTC

Many modifications to the linear JTC have been proposed and verified in recent years. Such improvements have produced the time-modulated joint power spectrum JTC [9], the position encoded complex JTC [25], the fringe-adjusted JTC [1], the phase-only JTC [7], and the nonlinear JTC incorporating a spatial-domain bipolar composite filter [26]. Further refinements to the nonlinear JTC include the nonlinear frequency-selective technique [16] and the multi-intensity imagery technique [5]. Although many research groups have investigated a wide range of modifications, the majority have worked only with software simulations. More recently, full implementations of JTC's incorporating such improvements have appeared which introduce nonlinearities into the system [10] or remove the autocorrelation term by a subtraction at the joint power spectrum [17].

Spectral Domain Thresholding. Additional intermediate nonlinear processing after the first Fourier transform, called spectral domain processing, can improve the performance of the JTC. Javidi [14] has shown the value of nonlinear transformations in the spectral domain. For highly nonlinear transformations, the high spatial frequencies are emphasised and the nonlinear JTC becomes more sensitive in discriminating between similar targets. One such transformation involves binarisation of the spectrum at a particular threshold level. The binary JTC uses a nonlinearity at the Fourier plane to reduce its joint power spectrum to only two values. It has been shown [12, 13] that compared to the linear JTC, the BJTC increases the resolution of the cross-correlation peaks providing higher peak intensities and narrower cross-correlation peak widths, and produces better discrimination between similar inputs. Although it is possible to analytically derive [12, 14] a nonlinear threshold function which maximises the cross-correlation peak intensity for a particular reference and input, this function is as large as the joint power spectrum itself and leads to unwieldy optical or electronic implementations. Currently, there is no general solution to the problem of efficiently identifying the optimal level for the easier-to-implement uniform threshold BJTC.

4 Experimental Results

All simulations were performed with the mathematical software MATLAB (The MathWorks, Inc.) and the verifications were conducted on a system employing an optical back transform. The illumination for this system was supplied by a frequency-doubled infrared YAG 0.5 mW laser, the inputs were encoded on a

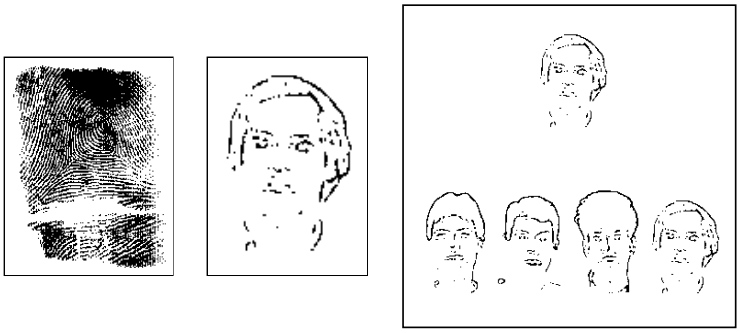

Fig. 3. Two sample input images, fingerprint no. 6 and face no. 31. Also, a complete 512×512 pixel input plane used in the multiple image experiments containing a reference and four inputs

high resolution LCD (liquid crystal display) panel from Sharp Electronics, and the joint Fourier spectrum sampled by a CCD (charge-coupled device) sensor.

For the thresholding experiments, each input plane signal consisted of two identical versions of the same image, displaced equally (but in opposite directions) from the origin. For the optical linear JTC experiments (Figs. 6 and 9) the images were placed side-by-side in the input plane and for the BJTC experiments (Figs. 7 and 10) the images were placed diagonally in the plane. This difference in layout may be deduced from the differing cross-correlation peak positions in each of the aforementioned figures. However, this did not introduce any secondary effects and the optical power in their respective cross-correlation terms may be compared directly.

There are noticeable differences between the simulated BJTC outputs and those obtained from the optical system. Although some errors are introduced by small lens aberrations and dust in the optical path, we found that the major contributing factor was oversampling of the joint power spectrum. The spectrum is sampled numerous times upon capture (by the CCD sensor, frame grabber) and redisplay (by the PC's video card, CCIR signal interface, LCD panel).

Figure 3 shows two images (one from each class) which were used for the particular results shown below, and also a complete input plane from one of the multiple input experiments.

4.1 Uniform Thresholding

Uniform thresholds were applied to the joint power spectra of the input planes described above. Figure 4 illustrates the operation of this threshold in the binarisation of a spectrum. The threshold level was varied and at several points the impulse response of the joint power spectrum was taken, thus producing a correlation output. The height of the cross-correlation peak (relative to the autocorrelation peak height) was measured at each stage and this dependency plotted.

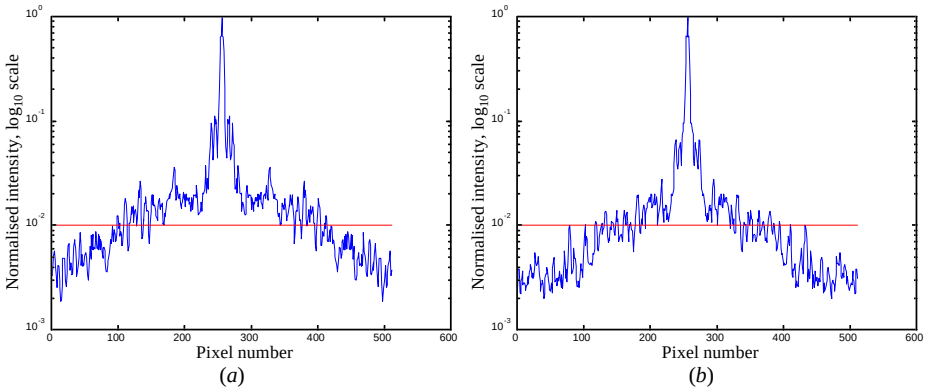

Fig. 4. Plot of two orthogonal projections (a) and (b) of the joint power spectrum of an input plane containing face no. 31, with overlaid optimal uniform threshold of 0.01 for visualisation. All values at or above the threshold are set to 1, all of those below are set to 0

A plot is shown in Fig. 5 of the cross-correlation peak height against threshold level for one of the face images. What is not evident from this figure is the shape of the cross-correlation peak at each point in the graph. Below a threshold of 10^{-1} the peak disappeared even though the mean energy in the output plane at the peak position was quite significant (see the right-most point on the curve). Within our region of interest, then, (between 10^{-3} and 10^{-1}) the threshold-level-versus-peak-height curve is uni-modal. From this we can say that a single maximum exists and that this maximum is well defined in that all points to the left of the maximum (within our region of interest) give rise to a negative first differential and all those to the right give rise to a positive first differential.

This graph in Fig. 5 reveals an optimal uniform threshold level for face no. 31 at 10^{-2}, denoting that the threshold should be set at 1% of the maximum peak in that joint power spectrum. All face image optimal thresholds were found in the range (0.01, 0.02). Also appearing in the plot of Fig. 5 is the height of the cross-correlation peak when the input plane with face no. 31 is processed with the linear, unthresholded, JTC. A comparison shows a BJTC improvement of 80% which was typical of the performance gains with the face set. Such simulations are verified in Figs. 6 and 7, which contain correlation plane signals of optically implemented linear and binary JTCs, respectively. It can be seen that the optical power in the cross-correlation terms of the thresholded JTC notably exceeds that of the unthresholded JTC.

Figures 8 through 10 contain similar results for fingerprint no. 6. This image has an optimal threshold of 10^{-4}, denoting that the joint power spectrum should be thresholded at 0.01% of the peak intensity. There was on average a 50% performance improvement for images of the fingerprint class (see Fig. 8), and a corresponding increase in optical power coupled into the cross-correlation terms of the optical BJTC (see Figs. 9 and 10).

4.2 Multiple Inputs

In order to properly quantify the performance of the optimally thresholded BJTC in multiple input environments (future work), comparisons must be made with a linear JTC implemented on an identical optical architecture. With this in mind, the discrimination ability of the linear JTC was measured both by simulation and optically on our system. Once again the height of the normalised cross-correlation peak was used to quantify performance.

Although in theory the JTC will produce the correct correlation signal regardless of the number of inputs, its discrimination abilities and correlation plane signal-to-noise ratio are severely diminished when the total optical energy in the input plane is increased relative to the reference image's energy. In these experiments the input planes consisted of one reference image spatially separated from a number of input images, such as that shown in Fig. 3. The number of inputs in each input plane ranged from 2 to 8.

Figure 11 shows the simulated correlation plane for the multiple input plane of Fig. 3. Although the discrimination ability of the JTC has not decreased (the 'correct' cross-correlation peak far exceeds the negligible cross-correlations between the reference and 'incorrect' inputs) it has dropped in intensity to 10% of the autocorrelation peak height (see vertical axis). The corresponding optical JTC output for the same input plane is shown in Fig. 12. This also shows dominant 'correct' cross-correlation peaks. However, compared to the single input results of Figs. 7 and 10 the autocorrelation term has increased significantly. It is also evident that on-axis cross-correlation terms between the four inputs have appeared to the left and right of the autocorrelation term. Both of these undesirable features (the increased autocorrelation term and input cross-correlation terms) contribute to a noisy correlation plane and threaten to lower the discrimination capabilities of this instance of the correlator.

It was found that although the linear JTC's discrimination ability remained high as additional inputs were introduced, the relative heights of the cross-correlation peaks fell below workable levels when more than four inputs were presented simultaneously. In these experiments we took a workable level to mean one where the 'correct' cross-correlation peak height was not less than 10% of the autocorrelation peak height and where the 'incorrect' peaks were not greater than 10% of the 'correct' peak.

5 Conclusions

We have investigated uniform thresholding in the spectral domain of a binary JTC in order to isolate the optimal threshold level for two image classes with fundamentally different spatial characteristics (fingerprints and faces). In simulations, the thresholds vastly improved the binary JTC's performance by increasing the normalised cross-correlation peak heights by on average 80% for faces and 50% for fingerprints, compared to the linear (unthresholded) JTC. These results were validated using a binary JTC employing an optical back transform.

For each image (from both classes) an optimal uniform threshold level does exist and this level is well defined. Although the optimal thresholds differed between image classes by a factor of 100, they were almost identical to the other members of their respective classes (each differed from the class mean by no more than 1% of the full threshold range). It is expected that this will enable a general solution to be found for predicting the optimal uniform threshold level given certain spatial characteristics of any input image. Such work is ongoing, as is a comparison between the optimal (but noiseless) technique of this paper and the more popular median and subset median [13, 14] thresholding techniques which are relatively insensitive to input noise.

These experiments have shown the value of nonlinear processing in the spectral domain of a binary JTC. It is expected that such spectral domain processing will enhance the intraclass discrimination performance of a multiple input JTC, the initial abilities of which have also been quantified for this paper.

References

[1] Mohammad S. Alam and Mohammad A. Karim, "Multiple target detection using a modified fringe-adjusted joint transform correlator", *Optical Engineering*, vol. 33, no. 5, pp. 1610–1617, May 1994.

[2] Henri H. Arsenault and Yunlong Sheng, *An Introduction to Optics in Computers*, volume TT8 of *Tutorial Texts in Optical Engineering*, section 1.4.1, pp. 8–10, SPIE Press, Bellingham, Washington, 1992.

[3] Ronald N. Bracewell, *The Fourier Transform and Its Applications*, chapter 6, pp. 98–126, McGraw-Hill Electrical and Electronic Engineering Series, McGraw-Hill, New York, second edition, 1978.

[4] David P. Casasent and Tien-Hsin Chao, eds., *Proceedings of Optical Pattern Recognition V*, volume 2237 of *SPIE*, Orlando, Florida, USA, March 1994.

[5] Zikuan Chen and Guoguang Mu, "Nonlinear joint transform correlator by interframe processing of multi-intensity imagery", *Optical Engineering*, vol. 35, no. 6, pp. 1746–1753, June 1996.

[6] L. J. Cutrona, Emmett N. Leith, C. J. Palermo and L. J. Porcello, "Optical data processing and filtering systems", *IRE Transactions on Information Theory*, vol. IT-6, pp. 386–400, June 1960.

[7] Peter S. Erbach, Don A. Gregory and Jeffery B. Hammock, "Phase-only joint-transform correlator: analysis and experimental results", *Applied Optics*, vol. 35, no. 17, pp. 3091–3096, June 1996.

[8] J. H. Feng, G. F. Chin, M. X. Wu, S. H. Yan and Y. B. Yan, "Multiobject recognition in a multichannel joint-transform correlator", *Optics Letters*, vol. 20, no. 1, pp. 82–84, January 1995.

[9] Thomas J. Grycewicz, "Applying time modulation to the joint transform correlator", *Optical Engineering*, vol. 33, no. 6, pp. 1813–1820, June 1994.

[10] Laurent Guibert, Gilles Keryer, Alain Servel, Mondher Attia, Harry S. MacKenzie, Pierre Pellat-Finet and Jean-Louis de Bougrenet de la Tocnaye, "On-board optical joint transform correlator for real-time road sign recognition", *Optical Engineering*, vol. 34, no. 1, pp. 135–143, January 1995.

[11] P. V. C. Hough, "Methods and measures for recognising complex patterns", US Patent No. 3069654, 18 December 1962.

[12] Bahram Javidi, Jun Wang and Qing Tan, "Multiple objects binary joint transform correlation using multiple level threshold crossing", *Applied Optics*, vol. 30, no. 29, pp. 4234–4244, October 1991.

[13] Bahram Javidi and Jun Wang, "Binary nonlinear joint transform correlation with median and subset median thresholding", *Applied Optics*, vol. 30, no. 8, pp. 967–976, March 1991.

[14] Bahram Javidi, "Nonlinear joint transform correlators", in Bahram Javidi and Joseph L. Horner, eds., *Real-time Optical Information Processing*, chapter 4, pp. 115–183, Academic Press, 1994.

[15] Miloš Klíma, Jiří Rott, Thomas Naughton and John Keating, "Joint transform correlation in security applications", in Larry D. Sanson, ed., *Proceedings of 31st Annual IEEE International Carnahan Conference on Security Technology*, pp. 77–81, Canberra, Australia, October 1997.

[16] Chung J. Kuo, "Joint-transform correlator improved by means of the frequency-selective technique", *Optical Engineering*, vol. 33, no. 2, pp. 522–527, February 1994.

[17] Chun-Te Li, Shizhuo Yin and Francis T. S. Yu, "Nonzero-order joint transform correlator", *Optical Engineering*, vol. 37, no. 1, pp. 58–65, January 1998.

[18] Thomas Naughton, "Fourier transform basics for optical image processing", Technical report, Department of Computer Science, National University of Ireland, Maynooth, Ireland, 1998. To appear.

[19] Edward L. O'Neill, "Spatial filtering in optics", *IRE Transactions on Information Theory*, vol. IT-2, pp. 56–65, June 1956.

[20] George L. Turin, "An introduction to matched filters", *IRE Transactions on Information Theory*, vol. IT-6, no. 3, pp. 311–329, June 1960.

[21] Anthony VanderLugt, "Signal detection by complex spatial filtering", *IEEE Transactions on Information Theory*, vol. IT-10, pp. 139–145, April 1964.

[22] Anthony VanderLugt, *Optical Signal Processing*, section 6.8, pp. 279–286, Wiley Series in Pure and Applied Optics, Wiley, New York, 1992.

[23] David Vernon, *Machine Vision*, chapter 6, pp. 118–139, Prentice Hall International, London, 1991.

[24] C. S. Weaver and Joseph W. Goodman, "A technique for optically convolving two functions", *Applied Optics*, vol. 5, no. 7, pp. 1248–1249, July 1966.

[25] Francis T. S. Yu, Guowen Lu, Mingzhe Lu and Dazun Zhao, "Application of position encoding to a complex joint transform correlator", *Applied Optics*, vol. 34, no. 8, pp. 1386–1388, March 1995.

[26] Francis T. S. Yu, Mingzhe Lu, Guowen Lu, Shizhuo Yin, Tracy D. Hudson and Deanna K. McMillen, "Optimum target detection using a spatial-domain bipolar composite filter with a joint transform correlator", *Optical Engineering*, vol. 34, no. 11, pp. 3200–3207, November 1995.

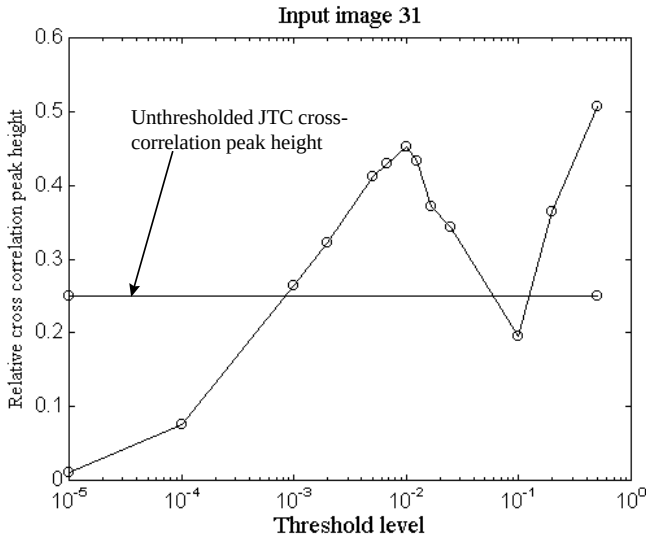

Fig. 5. Correlation peak vs. uniform threshold level, face no. 31

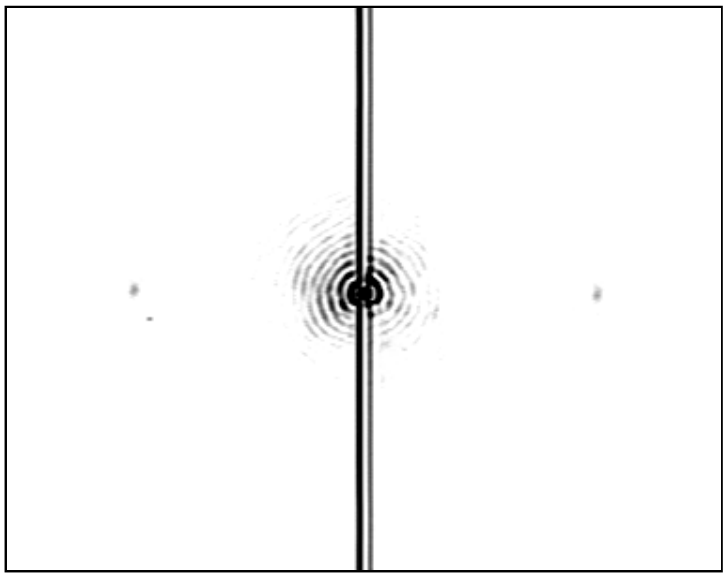

Fig. 6. Optical JTC output (unthresholded) for input plane containing face no. 31. Cross-correlation peaks appear to the left and right of the autocorrelation term

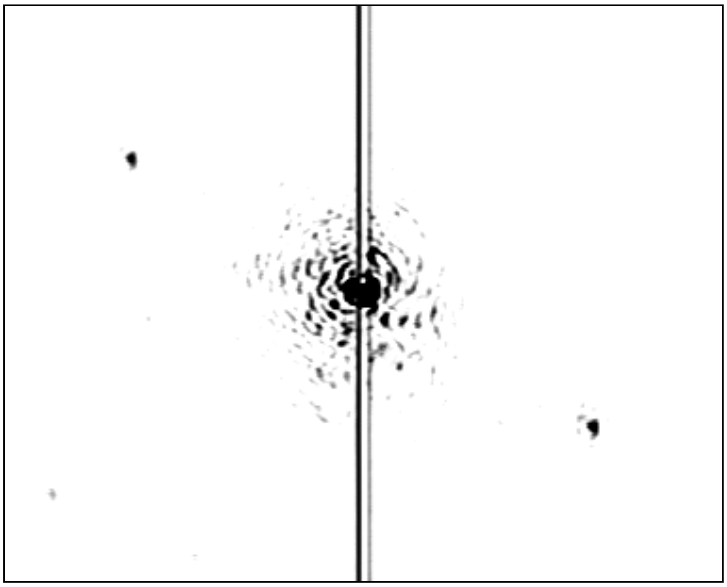

Fig. 7. Optical BJTC output (optimal uniform threshold of 10^{-2}) for input plane containing face no. 31. Cross-correlation peaks appear to the upper left and lower right of the autocorrelation term

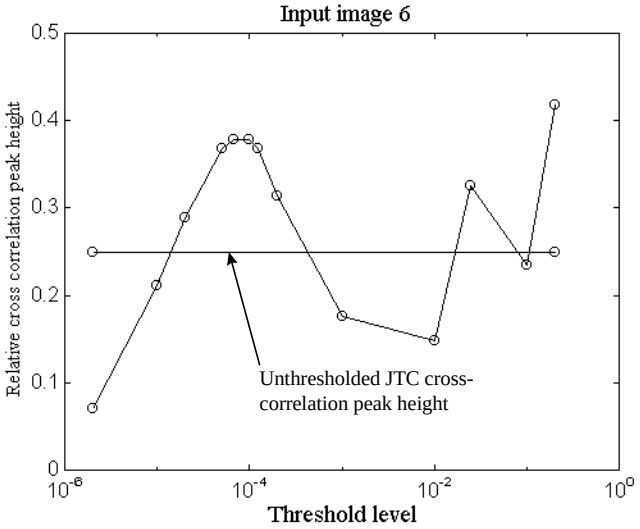

Fig. 8. Correlation peak vs. uniform threshold level, fingerprint no. 6

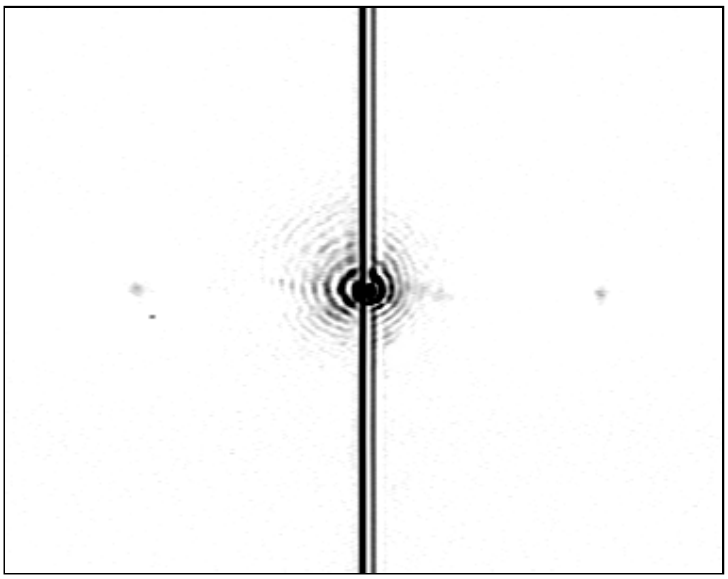

Fig. 9. Optical JTC output (unthresholded) for input plane containing fingerprint no. 6. Cross-correlation peaks appear to the left and right of the autocorrelation term

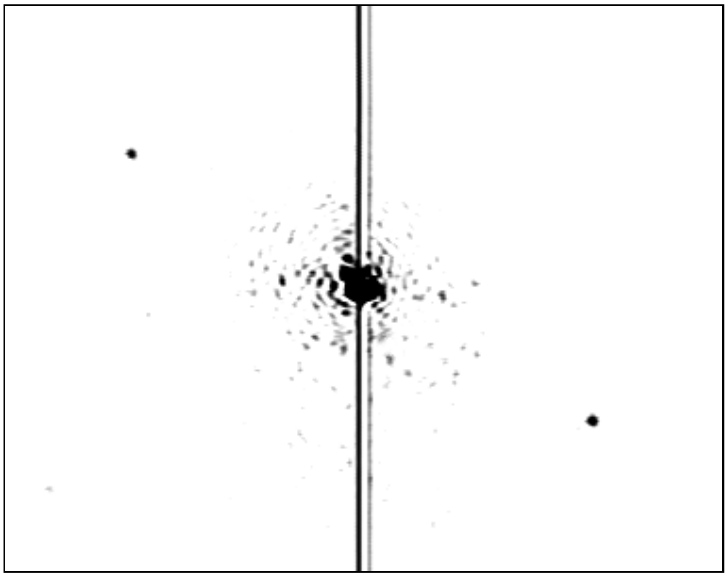

Fig. 10. Optical BJTC output (optimal uniform threshold of 10^{-4}) for input plane containing fingerprint no. 6. Cross-correlation peaks appear to the upper left and lower right of the autocorrelation term

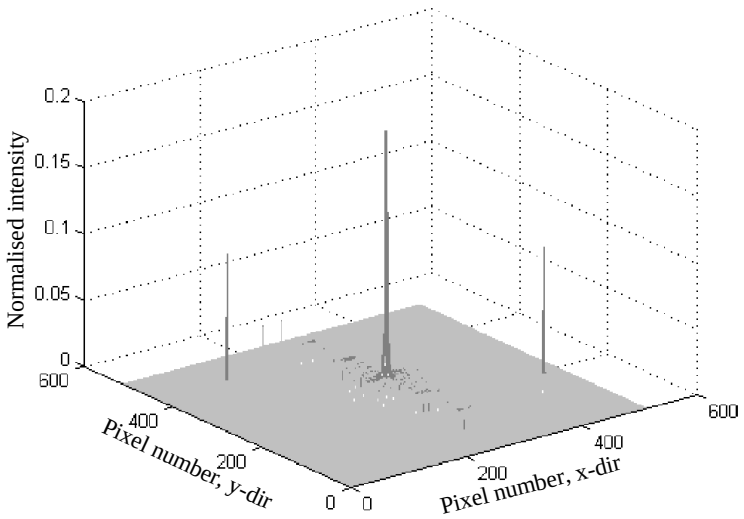

Fig. 11. Simulated JTC output for the multiple input plane from Fig. 3. Cross-correlation peaks appear to the left and right of the autocorrelation term

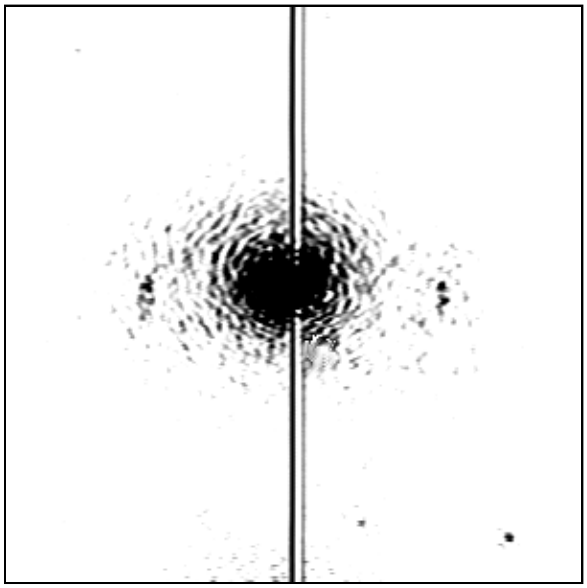

Fig. 12. Optical JTC output (unthresholded) for the multiple input plane from Fig. 3. Cross-correlation peaks appear at the extreme upper left and extreme lower right of the image. Note also the evidence of correlation between inputs, to the left and right of the dc term